Effect of localization–delocalization transition on thermoelectric properties of Bi$_2$Te$_2$Se topological insulator

L. Craco ; S. Leoni ✉

Check for updates

View Online

Export Citation

CrossMark

Applied Physics Reviews

Special Topic: Frontiers in energy materials research: novel measurement, modeling and processing approaches

Submit Today

AIP Publishing

AIP Publishing

Effect of localization–delocalization transition on thermoelectric properties of Bi₂Te₂Se topological insulator ⓕ

View Online   Export Citation   CrossMark

L. Craco[1,2] ⓘD and S. Leoni[3,a] ⓘD

AFFILIATIONS

[1] Institute of Physics, Federal University of Mato Grosso, 78060-900 Cuiabá, MT, Brazil

[2] Leibniz Institute for Solid State and Materials Research Dresden, D-01069 Dresden, Germany

[3] School of Chemistry, Cardiff University, Cardiff CF10 3AT, United Kingdom

[a] Author to whom correspondence should be addressed: LeoniS@Cardiff.ac.uk

ABSTRACT

The thermal transport properties of Bi₂Te₂Se topological insulators show a range of complex features. Large bulk resistivities coexisting with prominent Shubnikov–de Haas quantum oscillations and proximity to metallic states mark this p-band system as an unconventional topological quantum material. Here, using the density functional plus dynamical mean-field theory method, we show how localization–delocalization transition underpins the T-dependence of thermoelectric responses from room down to low temperatures. We present the implications of our many-particle analysis to resistivity, Seebeck coefficient, thermal conductivity, and Lorenz number and propose that related broadband systems close to electronic transitions could be of use in thermoelectrics.

High performance thermoelectric devices are essential to meet the requirements of global sustainable energy solution[1] due to their potential application for various power generation and refrigeration, which may involve novel green technologies.[2] Generally speaking, thermoelectric materials are a class of solid-state systems that can convert thermal energy into electricity for cooling or heating or recover waste heat and convert it into electrical power.[3] In these systems, a voltage drop can be induced in response to a temperature (T) gradient. Since the T-gradient usually affects both electronic and lattice degrees of freedom, optimizing thermoelectrics involves the fine-tuning of Seebeck coefficient (S) and the electrical (σ_{dc}) and thermal (κ) conductivities. In practice, what is needed for the application of thermoelectric devices is to produce materials with large conversion efficiency. This is usually quantified by the so-called figure of merit $ZT = \frac{\sigma_{dc} S^2}{\kappa} T$, where $\kappa = \kappa_{el} + \kappa_{ph}$, with κ_{el} and κ_{ph} being, respectively, the electronic and phononic (or lattice) contributions to the thermal conductivity. From ZT above, it is clear that a higher figure of merit is obtained by (independently) increasing the numerator or by decreasing the denominator;

the former is called thermoelectric power factor, Z_{PF}. The challenge problem for thermoelectric applications is to search for real materials,[4] where ZT approaches or exceeds unity at room temperatures. This can be done, for example, by controlling the transport of phonons and electrons in superlattices made up of two topological insulators Bi₂Te₃/Bi₂Te₂.₈₃Se₀.₁₇,[5] where $ZT \approx 1.4$ is achieved at 300 K or by decreasing $\kappa(T)$ as in nanocrystalline arrays of Bi$_x$Sb$_{2−x}$,[6] where similar ZT values were achieved at 373 K. Another promising direction is to search for off-stoichiometric Bi₂Te₂Se compounds, such as Bi₂Te₂.₄Se₀.₆[7] and Bi₂Te₁.₉₅Se₁.₀₅,[8] which, respectively, show a peak ZT of 0.94 at 423 K and 0.76 at 523 K. An additional interesting pathway is to maximize Z_{PF} employing complex bulk materials with strongly correlated electrons to enhance thermopower.[9–11] In this exciting perspective, an example is FeSb₂, which achieves a colossal Seebeck coefficient of 45 mV K^{-1} at low T.[12] In this work, we explore the role of electronic correlations on thermoelectrics by focusing on both Kondo and Mott regimes[13] of a bulk Bi₂Te₂Se topological insulator (TI). We argue that Mottness[14] is the key step in understanding the problem of
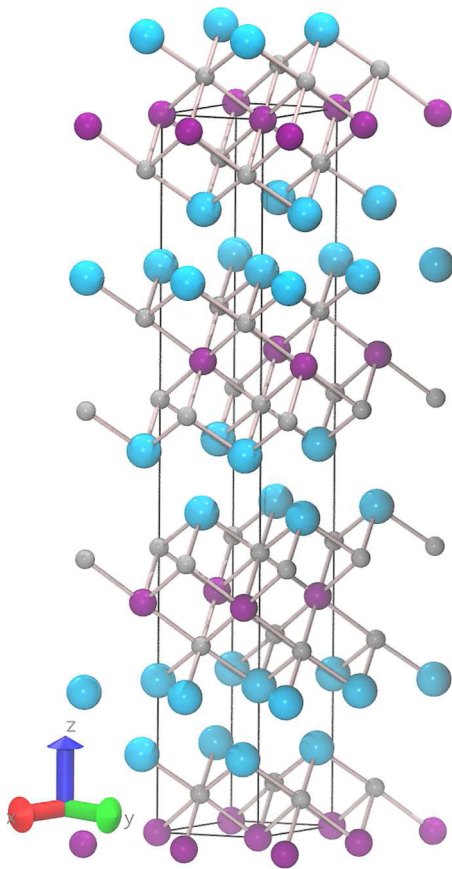
23 January 2024 13:16:00

FIG. 1. Crystal structure of the bulk Bi_2Te_2Se topological insulator: Bi (small gray), Te (large cyan), and Se (medium purple).

maximizing the electronic contribution to the thermoelectric power factor.

Theoretically, three-dimensional (3D) TIs are predicted to be bulk bandgap insulators characterized by a metallic surface state consisting of Dirac-like linear band dispersion.[15] Experimentally, however, most of the presently available TIs are conducting in the bulk. An exception, which is of interest here, is Bi_2Te_2Se (see Fig. 1), where large bulk resistivities[16–19] coexist with Shubnikov–de Haas (SdH) quantum oscillations[16,17,20] from surface states. The T-dependence and magnitude of dc-resistivity ($\rho_{dc} = 1/\sigma_{dc}$) in this TI appear to be sample[16,17] or carrier[18,19] dependent, showing variations between insulating and strange metal regimes. In insulating samples, the resistivity shows a semiconducting-like behavior above a characteristic temperature $T^\star \approx 50$ K[16,17] and becomes approximately constant below it. This saturated low-T regime[18] suggests the coexistence of spin–orbit-induced weak antilocalization and local-moment fluctuations in bulk Bi_2Te_2Se.

In an earlier study, we provided a many-particle description for the correlated electronic structure and dc transport of bulk Bi_2Te_2Se.[13] Our results, derived from reconstructed spectral functions in the bulk, are consistent with both photoemission and inverse-photoemission spectroscopy[21] as well as with resistivity

data,[16] showing that bulk Bi_2Te_2Se gives way to broadband Mott localization.[22] As in Ref. 23, here, we use a multi-channel, multi-orbital modeling (see the supplementary material for additional information) to unveil that Bi_2Te_2Se provides a rare opportunity to explore the role of correlated electronic excitations in tuning thermoelectric transport properties. To our best knowledge, this is a first attempt to uncover such complex features for a real topological p-band system. Finally, we show how the itinerant-localized duality (Mottness) makes for a sizable thermoelectric power factor in such a system and highlight the important role played by many-body electron–electron interactions effects[13,23] for thermoelectric materials.

Since the basic density functional plus dynamical mean-field theory (DFT+DMFT) formulation of coupled SO plus multi-orbital (MO) interactions has been introduced and used for real TI systems with good semiquantitative success,[13,26] we do not present it here but directly describe the correlated electronic structure and transport properties of bulk Bi_2Te_2Se. The abrupt electronic reconstruction across the Kondo–Mott electronic phase transition[13] is shown in Fig. 2. The atom-resolved, local-density-approximation plus dynamical mean-field theory (DFT+DMFT)[24] density-of-states (DOS) shows large-scale changes in the spectral weight transfer (SWT) at the critical phase boundary, 10.3 eV $< U_c <$ 10.4 eV.[27] As a consequence of Mottness, where the carriers have a dualistic itinerant-localized duality, the Kondo metal found for $U \leq 10.3$ eV is disrupted in insulating Bi_2Te_2Se, leaving us with a relative large range of pure linear DOS within the Se, Te-channels at $U = 10.4$ eV. Our results in Fig. 2 thus show that linear spectral functions near the Fermi energy (E_F) can be tuned by electronic interactions in the bulk. This is theoretical evidence that Coulomb repulsion[28] is a natural way to approach intrinsic topological Mott insulating regimes.[14] More importantly, only residual Bi valence band states span E_F in the channel-selective Kondo–Mott phase transition.[25] According to our theory, these residual Bi states are the microscopic origin of SdH quantum oscillations in the Bi_2Te_2Se TI,[16] while a large bulk resistivity is mostly due to effectively Mott-localized Te, Se-electronic channels.

The Seebeck coefficient, like the resistivity and thermal conductivity, can be computed within DMFT using the fully renormalized DFT+DMFT propagators.[29] Henceforth, we work in the orbital basis, which diagonalizes the one-particle density matrix in DFT.[30] This allows us to generalize the DMFT result[31] to the multi-channel, multi-orbital (MO) case relevant for Bi_2Te_2Se.[13] The general expressions used here for the Seebeck coefficient and electronic–thermal conductivity,[31] which, respectively, measure the mixed electrical–thermal correlations $[S(T)]$ and the heat–current correlations $[k_{el}(T)]$ at finite T, are

$$S(T) = \frac{1}{T}\frac{A_1(T)}{A_0(T)}$$

and

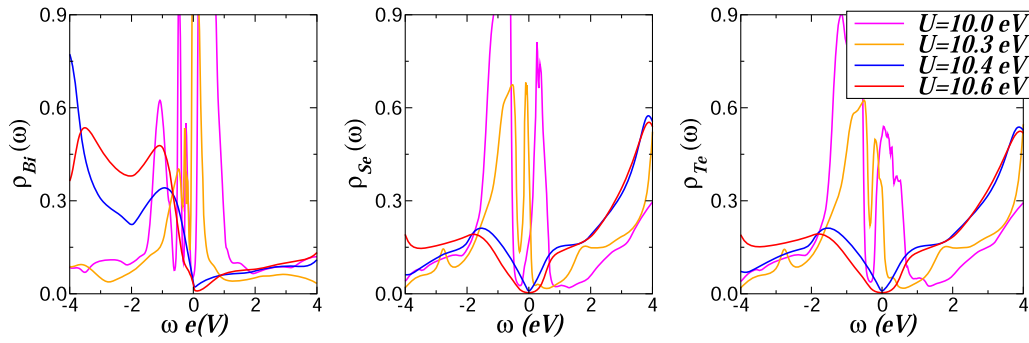$$k_{el}(T) = \frac{1}{T}\left(A_2(T) - \frac{A_1^2(T)}{A_0(T)}\right).$$

FIG. 2. Atom-resolved DFT+DMFT density-of-states (DOS) of Bi_2Te_2Se across the first-order localization–delocalization transition. Clear energy gap stabilization with increasing U goes hand-in-hand with a large-scale spectral weight transfer. Particularly interesting are the V-shaped spectral functions within the chalcogenide (Te, Se) electronic channels, with Dirac point-like minima at the Fermi energy, $\omega = E_F = 0$.

In our formalism,

$$A_n(T) = \zeta_n \sum_{\alpha,a} \int d\epsilon \rho_{\alpha,a}^{(0)}(\epsilon) \int d\omega \rho_{\alpha,a}^2(\epsilon,\omega)[-f'(\omega)](\omega - \mu)^n,$$

where $\zeta_n = \frac{e^2}{e^n\hbar} v^2$ and $a = x, y, z$ label the (diagonalized in the orbital basis) p bands of each atomic channel α [$\alpha = (1, 2, 3)$ corresponds, respectively, to (Bi, Te, Se)]. $\rho_{\alpha,a}(\epsilon,\omega) = -\frac{1}{\pi}\text{Im}[\omega - \Sigma_{\alpha,a}(\omega) - \epsilon_{\alpha,a}]^{-1}$ are the DFT+DMFT spectral functions, $\rho_{\alpha,a}^{(0)}(\epsilon)$ is the bare DOS, which encodes the details of the actual one-electron [Local Density Approximation (LDA)] band structure, and $\Sigma_{\alpha,a}(\omega)$ are the self-energies of all active p-channels. Finally, μ is the chemical potential and $f(\omega)$ is the Fermi function. As in Refs. 13, 26, and 32, the only approximation made here is to ignore the **k**-dependence of electron's velocity v. Given the complexity in Bi_2Te_2Se with three p bands on each atomic channel, this is an attractive scheme to compute thermoelectric transport properties of bulk TIs.

We now describe our transport results. In Fig. 3, we show the dc-resistivity, $\rho_{dc}(T) \equiv 1/A_0(T)$, of Bi_2Te_2Se for various U values. A T-dependent crossover from a high-T insulator to a low-T bad metal is seen for $U \leq 10.2$ eV. Clearly, this crossover scale is marked by the maximum of $\rho_{dc}(T)$. Our results show that 10.2 eV $\leq U < U_c$ yields a metallic behavior, in good qualitative agreement with Refs. 18, 19, and 33. In addition, in Fig. 2, the small spectral line shape for the Bi states shows power-law falloffs in the range -0.2 eV $< \omega < 0$ with a small residual DOS at E_F. Hence, at small but finite $T < T^\star$, the saturated regime[18] is expected to be totally incoherent in insulating samples. The drop of resistivity below $T^\star$ can be taken as a direct consequence of an increased mobility of residual electronic carriers that do not participate in the Mott state despite the increasing number of heavier carriers. Our theory thus suggests that the disappearance of the pseudogapped Bi valence band edge states by Fermi level tuning will eventually drive metallic Bi_2Te_2Se[18] into a maximally localized Mott state with a large bulk resistivity at low-T. Comprehensive semiquantitative accord with photoemission, inverse-photoemission, and dc resistivity (see Ref. 13) provides support to our view of tunable Kondo–Mott physics in the Bi_2Te_2Se TI. This gives us the confidence to use the DFT+DMFT spectral
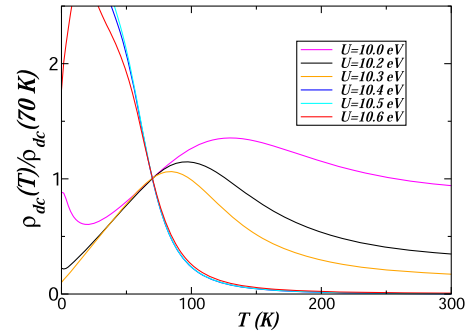

FIG. 3. dc-resistivities $[\rho_{dc}(T)]$ vs temperature for metallic and insulating phases of Bi_2Te_2Se, showing their evolution with increasing U. Notice the resistivity upturn for $U = 10.0$ eV at low T, a characteristic akin to Kondo systems.[32,34]

functions to explore room temperature thermoelectric responses of bulk Bi_2Te_2Se.

The T-dependence of the thermoelectric power $S(T)$ depicted in Fig. 4 shows clear fingerprints of electronic modification across the Kondo–Mott transition point. The fact that $S(T)$ changes the sign from positive (Kondo regime) to negative (Mott phase) is a signature of the multi-band character of transport linked to strong reorganization of MO electronic states at low energies.[13] Our results suggest a correlation-induced switching of electronic carriers in undoped Bi_2Te_2Se. As seen, the system spontaneously undergoes a charge reconstruction transition from a p- to n-type material when going from a Kondo metal to a Mott insulator. Remarkable as well is the appearance of isosbestic (crossing) points, a feature characteristic of correlated electron systems.[35] In the Mott phase, S is negative with a broad minimum at $T = 100$ K. However, in the Kondo regime, S changes sign from positive to negative at temperatures close to 100 K. This, in turn, suggests dramatically different emergent charge carrier localization near the Kondo–Mott phase transition. The smearing of low-T structures (which is a clear peak at $U = 10$ eV) in the Seebeck coefficient when approaching the first-order transition point is also noteworthy. A similar sign change and
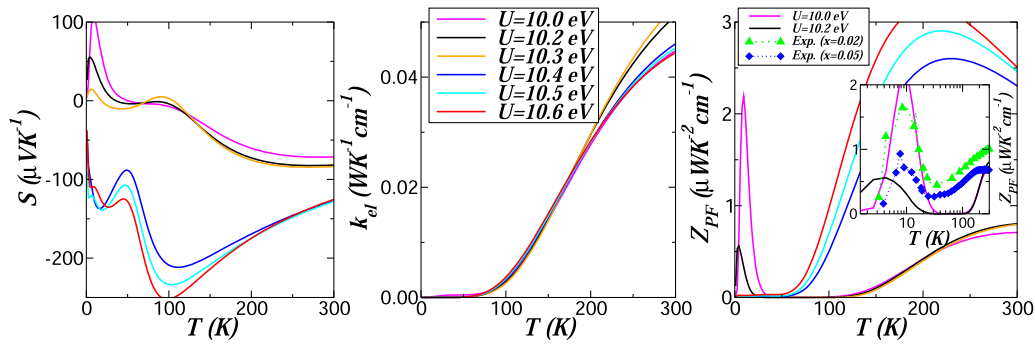
FIG. 4. Seebeck coefficient (left panel), thermal conductivity (center), and thermoelectric power factor (right panel) of Bi_2Te_2Se obtained using DFT+DMFT. Notice the change in sign in $S(T)$ across the correlation driven metal–insulator transition. Also interesting is the T-dependence of the thermoelectric power factor, Z_{PF}, showing high values at T close to 200 K. The inset of the right panel shows our theory–experiment between our DFT+DMF(MO-IPT) results and the power factor of another potentially interesting thermoelectric system, $Bi_{2-x}Ca_xSe_3$,[37] showing good qualitative agreement. The experimental curves have been rescaled to coincide with theory.

anomalous low-T peaks have been reported for doped Mott insulators[36] and observed in both n- and p-type Bi_2Se_3 TIs,[37] which might be a fingerprint common to correlated electron systems. While our results are not expected to reproduce all the main features seen in thermal transport experiments of bulk Bi_2Se_3 TI, our estimation of the crossing point in $S(T)$ for the parent compound Bi_2Te_2Se TI lies at a somewhat higher T than that found in Bi_2Se_3. This is caused by a stronger tendency to localization in Bi_2Te_2Se[13] compared to Bi_2Se_3.[26]

The electronic carriers generated from the thermal activation of low-energy excitations have a less pronounced effect in the electronic contribution to thermal conductivity, κ_{el}. As shown in Fig. 4, κ_{el} increases with temperature.[31,38,39] Below 100 K, the T-dependence of κ_{el} is surprisingly small, but the overall thermal conductivity we find for the Bi_2Te_2Se TI is comparable to the values measured in the normal state of iron-based superconductors.[39] Interestingly, while κ_{ph} usually displays a power-law T-dependence ($\kappa_{ph} \approx T^{-\beta}$, $0.75 < \beta < 0.95$),[40] κ_{el} for the Bi_2Te_2Se bulk crystal remains almost unaffected across the localization–delocalization transition, suggesting that its T-dependence is largely determined by a modest flow of thermal current due to MO, multi-channel-asymmetric quantum fluctuations of charge (particle/hole) carriers. Moving to the other transport properties, in the right panel of Fig. 4, we display the T-dependence of the thermoelectric power factor, $Z_{PF} = S^2/\rho_{dc}$.[37] As discussed for systems with SO coupling,[9] Z_{PF} is maximized in the vicinity of the insulator–metal transition. Here, we show in addition that this quantity for Bi_2Te_2Se increases with increasing U in the Mott phase at temperatures above 100 K. Meanwhile, within the Kondo regime, at temperatures above 100 K, Z_{PF} is almost independent of U, showing only a broad maximum at 300 K, consistent with the T-dependence of Z_{PF} found for $Bi_{2-x}Pb_xTe_2Se$ ($0 \le x \le 0.03$).[41] It is worth noting that, in this metallic phase, Z_{PF} displays in addition an anomalous low-T peak similar to that reported for Bi_2Se_3 TI,[37] and in our picture, this feature arises from weak antilocalization[42] induced by a strong SO interaction in the Bi-channel of Bi_2Te_2Se TI.[13]

As a final remark, historically, it is known that the electronic part of the thermal conductivity is related to carriers mobility
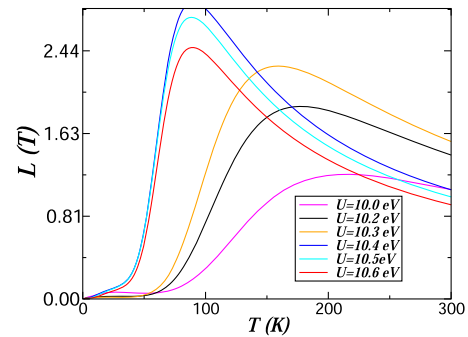

FIG. 5. Lorenz number L of Bi_2Te_2Se as a function of temperature for different values of on-site Coulomb repulsion, U. Notice the nonuniversal crossover region that approaches $L_0 = 2.44 \times 10^{-8}$ WΩ K^{-2} with increasing U.

through the Wiedemann–Franz relation: $k_{el}(T) = L\sigma_{dc}(T)T$, where L is the Lorenz number.[29] Although L is usually assumed to take a constant value $L_0 = 2.44 \times 10^{-8}$ WΩ K^{-2}, it, in fact, has significant temperature and material dependences.[43] Since this is true for TIs with strong spin–orbit (SO) coupling, in Fig. 5, we display its T-dependence for the Bi_2Te_2Se TI, showing that electronic interactions can push L $[\equiv k_{el}/(\sigma_{dc}T)]$ to values very close to L_0 in the Mott-localized regime, $U \ge 10.4$ eV. As shown in Fig. 5, $L(T)$ exhibits a remarkable nonuniversal[11] crossover region that approaches L_0 with increasing U up to the first-order transition point. Future experimental observation of T-dependent crossover in $L(T)$ would lend strong support to our theoretical work.

In summary, we have studied the role of localization–delocalization transition on the thermoelectric responses of the bulk Bi_2Te_2Se topological insulator. The anomalous character of the transport properties is interpreted in terms of atom- or channel-selective, multi-particle excitations. These arise from strong low-energy scatterings having its origin in the competition between selective-Mott localization and spin–orbit-induced

weak antilocalization in DFT+DMFT. Good semiquantitative agreement with spectroscopy and transport $[\rho_{dc}(T)]$ data above 70 K[16] in Ref. 13 as well as with a power factor of Ca-doped Bi_2Se_3[37] puts our mechanism for thermoelectrics on solid ground. Based on our results, we propose that related bismuth chalcogenide p-band systems with compelling experimental[44] and theoretical[23] evidence of intrinsic many-body effects would show up similar thermal transport features as found in this work. Taken together, our results provide a microscopic way to distinguish the correlated topological insulator from other possible bulk-metallic and bulk-insulating systems, which might be important for the potential applications of Bi-chalcogenide topological insulators not only for thermoelectric but also for charge–spin conversion devices.[45]

SUPPLEMENTARY MATERIAL

Detailed information regarding the Bi_2Te_2Se crystal structure, DFT calculations, total and projected DOS of Bi, Te and Se p-band states, DFT+DMFT calculations, multi-band, multi-orbital Hubbard model plus spin–orbit (SO) interaction Hamiltonian, and MO-IPT impurity solver is shown in the supplementary material.

ACKNOWLEDGMENTS

AUTHOR DECLARATIONS
Conflict of Interest

The authors have no conflicts to disclose.

Author Contributions

L. Craco: Conceptualization (lead); Data curation (equal); Formal analysis (equal); Investigation (equal); Methodology (equal); Software (equal); Validation (equal); Writing – original draft (equal). **S. Leoni**: Formal analysis (equal); Funding acquisition (lead); Resources (equal); Software (equal); Validation (equal); Visualization (equal); Writing – original draft (equal).

DATA AVAILABILITY

The data that support the findings of this study are available within the article.

REFERENCES

[1]G. J. Snyder and E. S. Toberer, Nat. Mater. **7**, 105 (2008).

[2]L. E. Bell, Science **321**, 1457 (2008).

[3]B. C. Sales, Science **295**, 1248 (2002).

[4]See, for example M. Markov, S. E. Rezaei, S. N. Sadeghi, K. Esfarjani, and M. Zebarjadi, Phys. Rev. Mater. **3**, 095401 (2019), and references therein.

[5]R. Venkatasubramanian, E. Siivola, T. Colpitts, and B. O'Quinn, Nature **413**, 597 (2001).

[6]B. Poudel, Q. Hao, Y. Ma, Y. Lan, A. Minnich, B. Yu, X. Yan, D. Wang, A. Muto, D. Vashaee, X. Chen, J. Liu, M. S. Dresselhaus, G. Chen, and Z. Ren, Science **320**, 634 (2008).

[7]G. Zheng, X. Su, T. Liang, Q. Lu, Y. Yan, C. Uher, and X. Tang, J. Mater. Chem. A **3**, 6603 (2015).

[8]B.-S. Kim, G. Lee, H.-J. Lim, J. Jang, J. E. Lee, B.-K. Min, S.-J. Joo, S. Park, B.-K. Ryu, and H. S. Lee, J. Electron. Mater. **49**, 5308 (2020).

[9]S. Hong, P. Ghaemi, J. E. Moore, and P. W. Phillips, Phys. Rev. B **88**, 075118 (2013).

[10]J. M. Tomczak, K. Haule, T. Miyake, A. Georges, and G. Kotliar, Phys. Rev. B **82**, 085104 (2010).

[11]V. Zlatić and J. K. Freericks, Phys. Rev. Lett. **109**, 266601 (2012).

[12]A. Bentien, S. Johnsen, G. K. H. Madsen, B. B. Iversen, and F. Steglich, Europhys. Lett. **80**, 17008 (2007).

[13]L. Craco and S. Leoni, Phys. Rev. B **85**, 195124 (2012).

[14]S.-L. Yu, X. C. Xie, and J.-X. Li, Phys. Rev. Lett. **107**, 010401 (2011); D. A. Pesin and L. Balents, Nat. Phys. **6**, 376 (2010).

[15]M. Z. Hasan and C. L. Kane, Rev. Mod. Phys. **82**, 3045 (2010); X.-L. Qi and S.-C. Zhang, *ibid.* **83**, 1057 (2011).

[16]J. Xiong, A. C. Petersen, D. Qu, Y. Hor, R. Cava, and N. Ong, Physica E **44**, 917 (2012).

[17]Z. Ren, A. A. Taskin, S. Sasaki, K. Segawa, and Y. Ando, Phys. Rev. B **82**, 241306(R) (2010).

[18]Z. Ren, A. A. Taskin, S. Sasaki, K. Segawa, and Y. Ando, Phys. Rev. B **84**, 165311 (2011).

[19]S. Jia, H. Ji, E. Climent-Pascual, M. K. Fuccillo, M. E. Charles, J. Xiong, N. P. Ong, and R. J. Cava, Phys. Rev. B **84**, 235206 (2011).

[20]A. A. Kapustin *et al.*, J. Exp. Theor. Phys. **121**, 279 (2015).

[21]Y. Ueda, A. Furuta, H. Okuda, M. Nakatake, H. Sato, H. Namatame, and M. Taniguchi, J. Electron Spectrosc. Relat. Phenom. **101–103**, 677 (1999).

[22]See G. Baskaran, arXiv:2308.01307 (2023), and references therein; See also, L. Craco, M. S. Laad, and S. Leoni, Sci. Rep. **7**, 2632 (2017).

[23]I. P. Rusinov, I. A. Nechaev, and E. V. Chulkov, JETP Lett. **98**, 397 (2013); I. Aguilera, C. Friedrich, and S. Blügel, Phys. Rev. B **100**, 155147 (2019), see also.

[24]G. Kotliar, S. Y. Savrasov, K. Haule, V. S. Oudovenko, O. Parcollet, and C. A. Marianetti, Rev. Mod. Phys. **78**, 865 (2006).

[25]A. Koga, N. Kawakami, R. Peters, and T. Pruschke, Phys. Rev. B **77**, 045120 (2008).

[26]L. Craco and S. Leoni, Phys. Rev. B **85**, 075114 (2012).

[27]The LDA+DMFT spectral functions were computed using fixed values for Hund's ($J_H = 0.5$) eV and spin–orbit ($V_{Bi} = 1.0$ eV) interaction.[13] In the multi-orbital many-particle problem, $U' = U - 2J_H$ is the inter-orbital Coulomb repulsion term.

[28]L. A. Wray, S.-Y. Xu, Y. Xia, D. Hsieh, A. V. Fedorov, Y. S. Hor, R. J. Cava, A. Bansil, H. Lin, and M. Z. Hasan, Nat. Phys. **7**, 32 (2011).

[29]*Properties and Applications of Thermoelectric Materials*, edited by V. Zlatic and A. C. Hewson (Springer, New York, 2009), p. 119.

[30]L. Craco, M. S. Laad, S. Leoni, and E. Müller-Hartmann, Phys. Rev. B **70**, 195116 (2004).

[31]C. Grenzebach, F. B. Anders, G. Czycholl, and T. Pruschke, Phys. Rev. B **74**, 195119 (2006).

[32]L. Craco, T. A. d. S. Pereira, and S. Leoni, Phys. Rev. B **96**, 075118 (2017).

[33]T. He *et al.*, Phys. Rev. B **100**, 094525 (2019).

[34]R. R. Urkude *et al.*, AIP Adv. **8**, 045315 (2018).

[35]D. Vollhardt, Phys. Rev. Lett. **78**, 1307 (1997).

[36]L.-F. Arsenault, B. S. Shastry, P. Sémon, and A.-M. S. Tremblay, Phys. Rev. B **87**, 035126 (2013).

[37]Y. S. Hor, A. Richardella, P. Roushan, Y. Xia, J. G. Checkelsky, A. Yazdani, M. Z. Hasan, N. P. Ong, and R. J. Cava, Phys. Rev. B **79**, 195208 (2009).

[38]J. K. Freericks and V. Zlatic, Phys. Rev. B **64**, 245118 (2001).

[39]M. Tropeano, I. Pallecchi, M. R. Cimberle, C. Ferdeghini, G. Lamura, M. Vignolo, A. Martinelli, A. Palenzona, and M. Putti, Supercond. Sci. Technol. **23** 054001 (2010); M. S. Kim, Z. P. Yin, L. L. Zhao, E. Morosan, G. Kotliar, and M. C. Aronson, Phys. Rev. B **84**, 075112 (2011).

23 January 2024 13:16:00

[40]S. S. P. Chowdhury, A. Samudrala, and S. Mogurampelly, arXiv:2305.15423 (2023).

[41]A. Léon *et al.*, Appl. Phys. Lett. **119**, 232103 (2021).

[42]R. K. Gopal *et al.*, Sci. Rep. **7**, 4924 (2017).

[43]G. S. Kumar, G. Prasad, and R. O. Pohl, J. Mater. Sci. **28**, 4261 (1993); J. Androulakis, Y. Lee, I. Todorov, D.-Y. Chung, and M. Kanatzidis, Phys. Rev. B **83**, 195209 (2011); Y.-L. Pei and Y. Liu, J. Alloys Compd. **514**, 40 (2012).

[44]M. Liu, C.-Z. Chang, Z. Zhang, Y. Zhang, W. Ruan, K. He, L.-L. Wang, X. Chen, J.-F. Jia, S.-C. Zhang, Q.-K. Xue, X. Ma, and Y. Wang, Phys. Rev. B **83**, 165440 (2011); J. Wang, A. M. Da Silva, C.-Z. Chang, K. He, J. K. Jain, N. Samarth, X.-C. Ma, Q.-K. Xue, and M. H. W. Chan, Phys. Rev. B **83**, 245438 (2011).

[45]J. Tian, C. Sahin, I. Miotkowski, M. E. Flatté, and Y. P. Chen, Phys. Rev. B **103**, 035412 (2021).

23 January 2024 13:16:00

2, 016102-6